Anal Bioanal Chem
DOI 10.1007/s00216-017-0262-5

PAPER IN FOREFRONT

Label-free visualization of nilotinib-functionalized gold nanoparticles within single mammalian cells by C_{60}-SIMS imaging

Anna N. Bloom[1] · **Hua Tian**[1] · **Christian Schoen**[2] · **Nicholas Winograd**[1]

Received: 16 December 2016 / Revised: 1 February 2017 / Accepted: 16 February 2017

Abstract Obtaining a comprehensive grasp of the behavior and interaction of pharmaceutical compounds within single cells provides some of the fundamental details necessary for more effective drug development. In particular, the changes ensuing in the carrier, drug, and host environment in targeted drug therapy applications must be explored in greater detail, as these are still not well understood. Here, nilotinib-functionalized gold nanoparticles are examined within single mammalian cells with use of imaging cluster secondary ion mass spectrometry in a model study designed to enhance our understanding of what occurs to these particles once that have been internalized. Nilotinib, several types of gold nanoparticles, and the functionalized combination of the two were surveyed and successfully imaged within single cells to determine uptake and performance. Both nilotinib and the gold particle are able to be distinguished and visualized in the functionalized nanoparticle assembly within the cell. These compounds, while both internalized, do not appear to be present in the same pixels of the chemical image, indicating possible cleavage of nilotinib from the particle after cell uptake. The method provided in this work is a direct measurement of uptake and subcellular distribution of an active drug and its carrier within a framework. The results obtained from this study have the potential to be applied to future studies to provide more effective and specific cellular delivery of a relevant pharmaceutical compound.

Keywords Secondary ion mass spectrometry · Targeted drug therapy · Nilotinib · Gold nanoparticles

✉ Anna N. Bloom
blooman06@gmail.com

[1] Department of Chemistry, The Pennsylvania State University, 104 Chemistry Building, University Park, PA 16802, USA

[2] Nanopartz Inc., 146 Barberry Place, Loveland, CO 80537, USA

Introduction

Obtaining a complete understanding of the location of a pharmaceutical compound within a biological system as well as the interactions of this compound at its site of action is crucial in garnering information about the system as a whole [1]. As such, the need continues to grow for the development of analytical methods that can produce information leading to new insights into drug behavior. Such information may ultimately determine the success of pharmaceuticals in the testing phases, reducing the 10–20-year timeline and $2.5 billion cost currently attributed to the discovery and development of a novel compound [2].

The importance of expanded understanding within this area of research is so great that some scientists have defined successful compounds using confirmation of three parameters: the target site of action must be exposed to the compound over a desired length of time, the drug must bind to and engage with the pharmacological target as intended, and the anticipated pharmacological activity must be expressed, eliciting the response of interest. Although each of these fundamental aspects is imperative, its independent presence is not a direct measure of success [3]. Therefore, it is important to test for each of these properties individually, ideally with use of a single analytical technique.

Targeted drug therapies have become a more prominent approach in ensuring that these three parameters are successfully met, by defining the exact location of where pharmaceutical compounds interact within the body and when the target is engaged. Successfully administering specific compounds only at desired locations results in the administration of lower dosages, which culminates in lower side effects, ultimately leading to more desirable patient adherence as well as decreased cost when compared with the established medications on their own.

Nanoparticles of many varieties provide an interesting platform for such targeted drug delivery approaches, as they can be tuned to exhibit altering behaviors within the body. It is possible

Published online: 10 March 2017

to change the properties of the particles rather than the active compounds themselves in an effort to more precisely regulate when and where compounds are released. Increased efficiency of delivery, increased solubility, greater stability in vivo, and more advantageous biodistribution are just several of the advantages these therapies provide over traditional, free drug administration [4–6]. The high biocompatibility and low toxicity of gold nanoparticles (AuNPs) make them a particularly interesting target of investigation [7, 8]. Many methods for manufacturing AuNPs exist, allowing careful control over the size, shape, surface functionalization, and state of aggregation, providing researchers with a powerful tool in designing particles that showcase the desired properties. Even the elusive crossing of the blood–brain barrier has been achieved with these particles, making it possible to deliver medications to portions of the brain that had not been previously reached [9].

Although much research has been centered around AuNPs within biological systems, it is currently difficult to use one technique to obtain all the required information for thoroughly understanding the nature of the interactions between AuNPs, pharmaceutical compounds (or other functionalization), and the surrounding environment. In addition, there is little insight surrounding the behavior of the AuNP with respect to its functionalization. Although techniques such as scanning electron microscopy and fluorescence microscopy can identify the particle or the functionalization individually, little is known about how the assembly of particle and functionalization behave in the cell. It is still unclear if these components of targeted drug delivery applications remain bound to one another or, if cleavage occurs, how the behavior of the compound and/or particle is affected. In addition, current investigations have focused on measuring the uptake of the gold itself, rather than that of the functionalization. It is the carrying capacity of these particles, rather than the amount of gold, which is important in targeted drug delivery, and so this avenue of inquiry must also be pursued [10].

Many existing studies rely on the concentration of the compound of interest in cellular plasma for an indication of how much drug reaches the target, though this marker is not always a definitive indicator of that information [11]. Other common analytical techniques such as fluorescence microscopy, high-performance liquid chromatography, and matrix-assisted laser desorption ionization mass spectrometry, which are used to probe the success of pharmaceutical compounds in various forms, rely on the use of labels or the quantification of large numbers of cells [12] to understand the interactions between the cellular host and the pharmaceutical compound. In these cases, there is the potential for the chemistry of the compound to be changed, and subcellular localization is not always possible. In addition, when labels are used, only the compounds of interest that have been tagged can be visualized.

The secondary ion mass spectrometry (SIMS) technique has the ability to produce both chemical and spatial information simultaneously, without the use of a matrix or label. These aspects allow the possibility of identifying not only the location of the molecular ion of the compound of interest intracellularly but also any relevant metabolites and chemical changes to the cells [13]. This ability to map all compounds over a specific area has the potential to aid in the elucidation of the mechanisms of action and behavior the compound has been once internalized into the cell, as well as the interaction between the drug carrier, pharmaceutical compound, and host environment.

The study of single cells as well as cells doped with exogenous compounds is not without precedent. Research has showcased the ability of SIMS to visualize fluorescent dyes [14], pharmaceutical compounds [13, 15], nanoparticles [15–20], and other exogenous compounds within mammalian cells successfully. The work reported here extends what was learned from initial model systems involving the cluster SIMS visualization of fluorophore-functionalized AuNPs [15] to a more medically relevant scheme involving drug-functionalized AuNPs.

Nilotinib ($C_{28}H_{22}F_3N_7O$, molecular weight 529, chemical structure shown in Fig. 1) was chosen as the model compound of interest to observe within cells. It has been found to produce a strong, characteristic SIMS signal within standard biological matrices, making it readily identifiable in biological systems, while still maintaining relevance in medicinal research. It has been previously approved for the treatment of imatinib-resistant chronic myelogenous leukemia and functions by inhibiting a class of protein (c-Abl) [21]; c-Abl is a human cytoplasmic and nuclear protein tyrosine kinase that has been shown to participate in various cell processes, including cell division, differentiation, adhesion, and stress response.

Higher levels of c-Abl are closely associated with Parkinson's disease, resulting in increased interest in this compound as a potential treatment option. Under normal circumstances the protein parkin is responsible for labeling nonessential and dysfunctional proteins and mitochondria for degradation. Increased levels of c-Abl inhibit parkin, resulting in an accumulation of α-synuclein and damaged mitochondria, which, in turn, may cause decreased dopamine signaling and the formation of harmful aggregates within the brain. These factors are characteristic markers of Parkinson's disease [22, 23].

Although low concentrations of nilotinib may cross the blood–brain barrier when nilotinib is administered orally [24], it is still necessary to explore avenues, such as functionalization onto AuNPs, that result in greater uptake and lesser side effects of nilotinib within the brain. Although nilotinib has not been examined on AuNPs, it has been probed on hybrid protein kinase inhibitor/polymer nanoparticles [25]. In addition, other classes of tyrosine kinase inhibitors functionalized onto AuNPs have been studied [26–28], with some research suggesting an increase in effectiveness when they are coadministered with gold [29].

Although the molecular biology, pharmacology, and tissue distribution of nilotinib are well characterized, little is known about its potential in targeted drug therapies using a nanoparticle carrier. Here, we report the first example of the study of

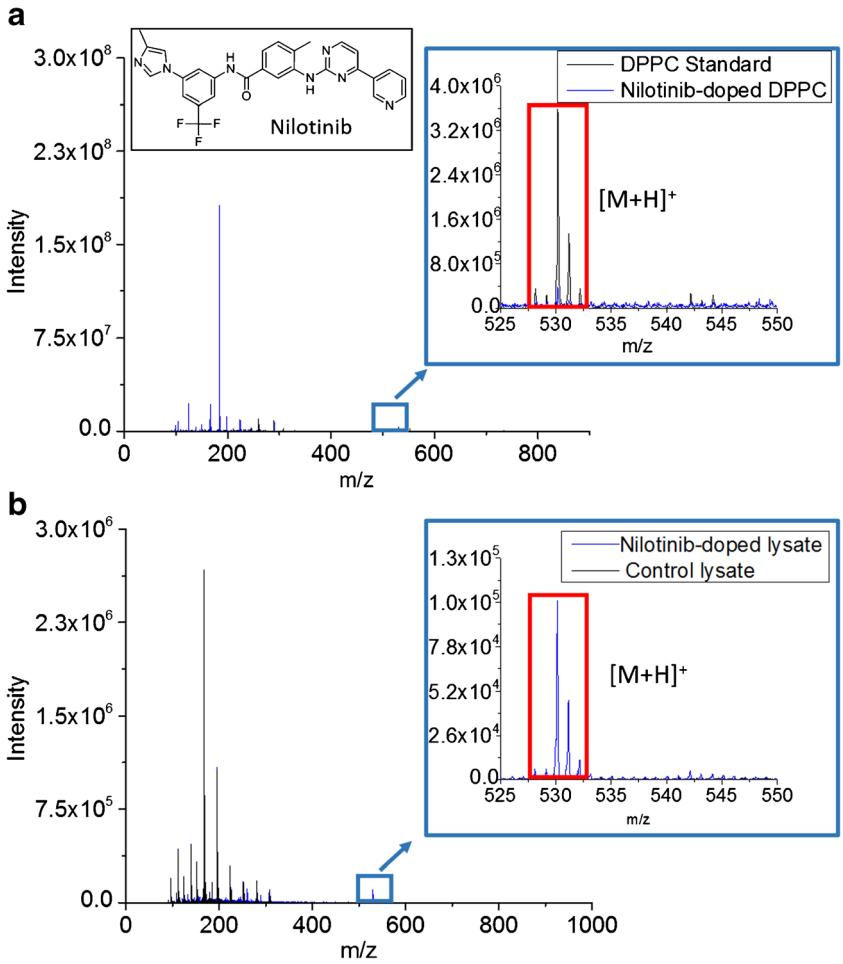

Fig 1 Spectral comparison of **a** nilotinib standard spectrum and nilotinib in a 1,2-dipalmitoyl-*sn*-glycero-3-phosphocholine (*DPPC*) matrix and **b** layer 5 of RAW 264.7 lysate and RAW 264.7 lysate doped with 50 μM nilotinib. These spectra show that nilotinib can be visualized in a cellular environment and that no inherent, biological peaks interfere with $[M + H]^+$ of nilotinib. The spectra were acquired in positive polarity

pharmaceutical-compound-functionalized AuNPs within a model mammalian cell line using cluster SIMS. We survey the uptake and distribution of both AuNPs and nilotinib individually, before investigating them simultaneously as a drug-functionalized nanoparticle assembly. This study provides unique information about a complex drug delivery platform, providing insight into the behavior of the system as a whole that has previously been difficult to ascertain with a single technique. Mainly, this study proves that both compounds of the model functionalized AuNP system are successfully internalized by the cell and can be studied with respect to one another, making it possible to draw conclusions about the location and attachment to one another. The information gained from this work has the potential to be applied to future targeted drug therapy applications, in the hope of making them more effective (aiding in the design of effective drugs).

Materials and methods

Cell culture

RAW 264.7 cells, macrophage-like cells derived from tumors induced in mice by the Abelson murine leukemia virus, were maintained in Dulbecco's modified Eagle's medium (DMEM; 1×, Corning Cellgro, Manassas, VA, USA) with 10% fetal bovine serum (Gibco by Thermo Fisher Scientific, Carlsbad, CA, USA) and 5% penicillin–streptomycin (100×, Corning Cellgro, Manassas, VA, USA) in an incubator at 37 °C and with 5% CO_2. After they had been rinsed with Dulbecco's phosphate-buffered saline (DPBS; Corning Cellgro, Manassas, VA, USA), cells were detached from culture flasks with use of a cell scraper and cultured onto 5 mm × 5 mm silicon chips. These chips had been cleaned by sonication in chloroform, acetone, methanol, and purified water for 5 min each, consecutively. Cells were allowed to grow for 24 h before administration of any compounds.

Drug standards study

Reference spectra of all compounds tested were acquired in the drop deposited state. Compounds were also studied within a lipid matrix, in which the compound was added to 1,2-dipalmitoyl-*sn*-glycero-3-phosphocholine (DPPC; Avanti Polar Lipids, Alabaster, AL, USA) dissolved in chloroform to 50 μM concentration. This was done to confirm visibility within a lipid matrix. Each compound was also observed at 50 μM concentration within a cell lysate. The lysate was obtained

through mechanical lysis. All samples were spin coated onto silicon chips (3000 rpm; acceleration, 500 rpm for 30 s) and allowed to dry under ambient conditions. Standards of the lysate and DPPC were prepared and reviewed under conditions comparable to those for the doped samples.

Nanoparticle studies

All nanoparticles were provided by Nanopartz (Loveland, CO, USA) and studied without modification within cells. After 24 h of growth on silicon chips, cells were exposed to the desired nanoparticle concentration (5.00×10^{10} particles per milliliter) in starvation medium (DMEM 1× without fetal bovine serum) overnight. Cells were also inspected after incubation in starvation medium without nanoparticles to confirm that they remained viable. The nanoparticles investigated include 10-nm diameter × 41-nm length cell uptake polymer functionalized gold nanorods (10 nm × 41 nm nanorods), 20-nm cell uptake polymer functionalized gold nanospheres (20 nm nanospheres), 10-nm diameter × 41-nm length negative polymer functionalized gold nanorods (negative 10 nm × 41 nm nanorods), and 5-nm nuclear uptake polymer functionalized gold nanospheres.

The 10 nm × 41 nm gold nanorods were manufactured by a modified Murphy cetyltrimethylammonium bromide (CTAB) method resulting in highly monodisperse gold nanorods. The length and width standard deviations were measured to be better than 10%. For the uptake polymer functionalization, the CTAB concentration in solution was reduced to 1 mM by dialysis and a proprietary ionic 5-kDa amine polymer was used to replace the CTAB. The final zeta potential was +30 mV. The negative polymer functionalized gold nanorods were manufactured by a standard citrate reduction method. These too were functionalized the same way but with use of proprietary ionic 5-kDa carboxyl-based polymer instead of CTAB. The final zeta potential was -25 mV.

The 20-nm spheres were manufactured by a proprietary citrate reduction resulting in highly monodisperse spheres with a standard deviation of better than 6%. These spheres were coated with the same polymer as the nanorods by the same method. The 5-nm spheres were manufactured by a proprietary citrate reduction resulting in highly monodisperse spheres with a standard deviation of better than 20%. These spheres were coated with a nuclear uptake peptide (nuclear localization sequence).

Exposure to pharmaceutical compounds

Nilotinib was provided by Novartis Pharmaceuticals (San Francisco, CA, USA) and was studied within cells without modification. Cells that had been allowed to grow for 24 h were exposed to the desired concentration (1–150 μM) of nilotinib for 60 min in starvation medium (DMEM 1× without fetal bovine serum) before fixation. In all cases, cell morphology was monitored to ensure viability of the sample on doping.

Exposure to nilotinib-functionalized gold nanoparticles

The 20-nm cell uptake polymer/nilotinib-functionalized gold nanospheres (Nanopartz, Loveland, CO, USA) were studied within cells without modification. After 24 h of growth on silicon chips, cells were exposed to the desired nanoparticle concentration (5.00×10^{10} particles per milliliter) in starvation medium (DMEM 1× without fetal bovine serum) overnight.

The 20-nm spheres were modified with a cell uptake polymer (branched) that ionically embeds the nilotinib. The increase in size was measured by dynamic light scattering to be 23 nm, with a zeta potential of -18 mV.

Sample preparation

After the completion of exogenous compound treatment, the cell-covered silicon chips were removed from the medium. Cells were washed twice in DPBS that had been warmed to 37 °C. Samples were then chemically fixed at 5 °C with formalin (1:10 dilution buffered, Thermo Fischer Scientific, Kalamazoo, MI, USA) for 15 min. After fixation, cells were washed three times in DPBS to remove excess fixing solution, followed by a 1-min rinse in 0.015 M ammonium formate (pH 7.3; Alfa Aesar, Tewksbury, MA, USA). Ammonium formate was used to minimize variation from accepted cellular preparation methods that use this solution to remove residual salts [30]. The samples were allowed to dry in air before insertion into the SIMS instrument. The cross-linking of the cellular proteins that occurs as a result of formalin fixation imparts the rigidity of the cell structure.

Cluster secondary ion mass spectrometry

Cluster SIMS characterization was performed with a J105 3D chemical imager (Ionoptika, Southampton, UK) equipped with a 40-keV C_{60}^+ source that has been described previously [31]. Samples were studied at room temperature.

Images were acquired with positive polarity with use of a C_{60}^+ beam with a 500-nm focused spot size, resulting in 500-nm lateral resolution. This resolution was measured with use of the edge of a 600-mesh grid by a secondary electron detector that is built into the instrument. The field of view for all images was 100 μm × 100 μm, containing 256 × 256 pixels. Each chemical image is the result of exposure of the sample surface to an ion dose of 3.4×10^{13} ions per square centimeter. Subsequent images were acquired as a function of sample depth, referred to as a depth profile, resulting in multiple layers that span the depth of the sample. In experiments using 3D representations, layer 1 corresponds to the first image acquired, indicating the surface of the sample, whereas subsequent layers represent additional acquisitions of the same area with the same experimental parameters. The acquisition time for each chemical image was 25 min.

Data were processed by Analyze from Ionoptika. Chemical images were created by the mapping of the mass ranges of the compounds of interest. In the cases involving statistical analysis, regions of interest were selected by our choosing either the cellular area or 15 × 15 pixels in a particular area. The mass ranges of the compounds (*m/z* 184.07 Δm = 0.05, *m/z* 196.96 Δm = 0.025, all others Δm = 0.20) of interest were selected, and the ratios of those counts were compared between the sample with and the sample without exposure to AuNPs or nilotinib to determine if increased levels were present in doped cells. In each case, at least three different cells were compared to allow the calculation of averages and standard deviations.

Results and discussion

Determining detection capabilities of nilotinib in standard matrices

Not all compounds can be readily detected by cluster SIMS, and so ensuring the detection capabilities of nilotinib within a standard matrix was necessary. First, a standard spectrum of nilotinib was obtained as a reference. DPPC served as a simplified composition of a model cellular membrane to indicate the presence of possible matrix effects or signal suppressions. The ability to detect the isotope pattern of the protonated nilotinib molecular ion (*m/z* 530.19, $[M + H]^+$) can be seen in Fig. 1a.

Following examination in a standard matrix, nilotinib was assessed in a cell lysate to ensure that the peak corresponding to the protonated molecular ion was distinguishable from the cellular material and exclusive to the exogenous compound. The unique nature of the protonated molecular ion of nilotinib within the cellular environment can be seen in Fig. 1b. This peak illustrates that the signal observed at this *m/z* can be attributed to the drug alone, as no such peak can be observed in a standard cell lysate spectrum.

The capacity to detect the protonated molecular ion rather than fragments provides evidence that nilotinib can be identified in its active form, which is its molecular form. Although this compound has been shown to produce 20 distinct human metabolites, none contribute to its pharmacological activity, nor are they a major component of human plasma on administration [32]. It is for this reason that these metabolites were not part of this study.

Nilotinib in RAW 264.7 cells

Once it had been established that nilotinib could be successfully observed within control matrices composed of DPPC and cellular lysate, applications within RAW 264.7 cells were performed. RAW 264.7 cells were used as a model cell system because of their tendency to internalize compounds readily. A variety of concentrations were studied (5–100 μM) to determine the dynamic range and limits of detection. At 100 μM, the cell shapes became distorted, implying that this concentration was too great to be used in work involving healthy cells. In cells exposed to concentrations below 5 μM, the protonated molecular ion signal could no longer be confidently distinguished from the noise level.

The chemical images in Fig. 2 show cells exposed to 25 μM nilotinib for 3 h. The phosphocholine (PC) head group at *m/z* 184.07 is a well-established marker [33] of the cellular region, as it is a major fragment of membrane PC lipids. The protonated molecular ion of nilotinib (*m/z* 530.19) is used as a marker for drug presence. On the topmost layer of the cell (layer 1), a strong PC head group signal is evident, revealing the regime of the cellular region. Here, there is very little signal corresponding to the protonated nilotinib molecular ion, indicating that it is outside the detection limits on the exterior of the cell membrane.

By the acquisition of the third chemical image within this sample ("layer 3," total ion dose 1.0×10^{14} ions per square centimeter), the upper portions of the cell have been etched away and the interior (approximate depth 100 nm into the cell), including the cytoplasm, becomes visible. The chemical and structural features of the internal regions of the cell can now be seen. Signal corresponding to nilotinib can now be clearly visualized within the cell. The distribution of the PC head group and that of the protonated molecular ion co-localize with one another, demonstrating successful uptake within the cell. Regions of higher counts of nilotinib, as illustrated by circles in Fig. 2, also appear to be present, suggesting that subcellular localization may be occurring. In areas containing nilotinib in visually concentrated areas, the ratio between nilotinib counts and the counts of the PC head group is 3.0 ± 0.9, whereas this ratio is 0.5 ± 0.4 in areas containing nilotinib in less visually intense areas. The PC head group was chosen for comparison, as it is a uniform and consistent component of cellular material. Because of the possibility of matrix effects and the difficulty of a quantitative study, which are inherent to the SIMS technique, no conclusions regarding internal concentration can be drawn. As nilotinib is believed to interact with lysosomes [34], it may be possible that such an accumulation is what is being shown; however, without secondary verification no concrete conclusions can be drawn yet.

The protonated molecular ion signal continues through the cell, and by layer 12 of the depth profile (total ion dose 4.1×10^{14} ions per square centimeter) it is apparent that nilotinib is internalized; however, if any of the compound does penetrate into the nuclear region, as defined by the void in the PC head group signal in the interior of the cellular area, it is below the detection limit of the instrument. On the basis of the known behavior of nilotinib, no interactions with the nucleus are expected [32]. The depth profile imaging clearly shows the shrinking of the cellular area throughout the acquisition, which is consistent with the consumption of cells under C_{60} beam etching. On the basis of previous studies, the etching rate throughout the organic matter within the cell can be assumed to remain constant [35].

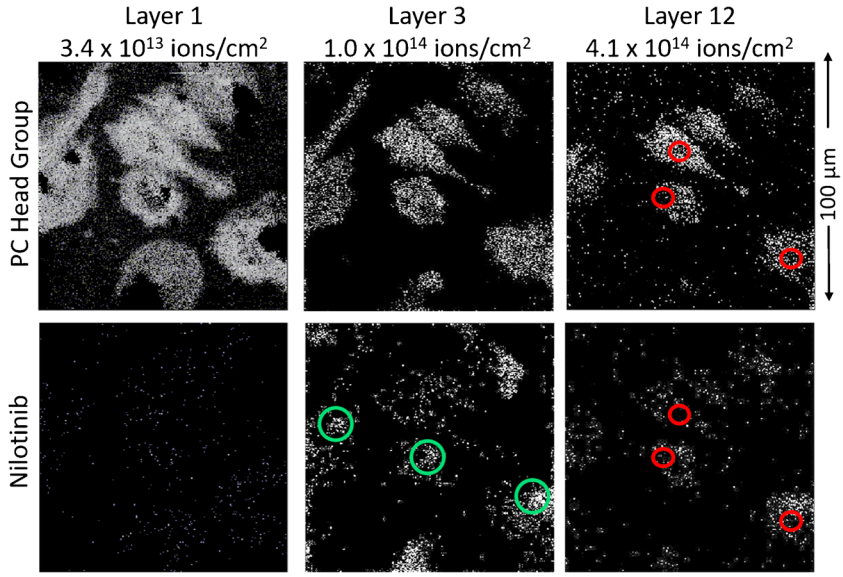

Fig. 2 Positive secondary ion mass spectrometry (SIMS) chemical images of formalin-fixed RAW 264.7 cells exposed to 25 μM nilotinib for 3 h. The nilotinib protonated molecular ion signal is present once the internal regions of the cell have been exposed. These chemical images show the cellular uptake and potential subcellular accumulation of nilotinib within these cells (*green regions*). The *red regions* show the void in the phosphocholine (*PC*) head group attributed to the nuclear region. The PC head group is defined by m/z 184.07 and the nilotinib protonated molecular ion is defined by m/z 530.19. All images are 100 μm × 100 μm

As it is important to determine that concentrations of this compound that are close to therapeutically relevant levels can be detected [36], cells were probed after exposure to 5 μM nilotinib for 3 h. The chemical image in Fig. 3 shows that although the signal levels are low, it appears that a certain level of aggregation of nilotinib is present in the cellular region, making it possible to assign co-localization of this drug with areas defined as belonging to the cell. Although there is some diffuse signal in areas surrounding the cell, this is explained by residual compound not being removed by washing as well as by background noise.

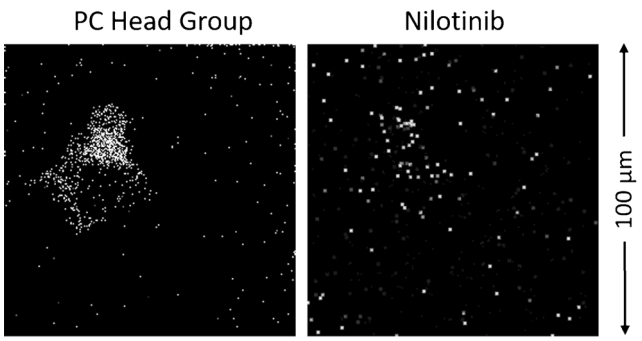

Fig. 3 Positive SIMS chemical images of formalin-fixed RAW 264.7 cells exposed to 5 μM nilotinib for 3 h. The chemical images shown are for layer 9 of the sample, corresponding to a total ion dose of 3.1×10^{14} ions per square centimeter. Co-localization of the cellular signal (m/z 184.07) and signal of the protonated molecular ion of nilotinib (m/z 530.19) is visible. All images are 100 μm × 100 μm

Detection of nanoparticles in RAW 264.7 cells

Several varieties of AuNPs were studied to determine if behavioral differences in particle uptake could be observed. The size, shape, zeta potential, and functionalization of these particles has a profound impact on their behavior, and it was of interest if these differences could be observed with SIMS. It is believed that the electrostatic interactions surrounding the particle are what bring it close to the cell surface, whereas the hydrophilic and hydrophobic interactions aid in the recognition of relevant domains on the surface [37]. There is evidence that nanorods are more effective in targeted drug delivery, as they adhere more effectively to cell surfaces, and so they were included in this study [38]. Several different nanoparticles were investigated, including 10 nm × 41 nm cell uptake polymer functionalized gold nanorods, 20-nm cell uptake polymer functionalized gold nanospheres, and 10 nm × 41 nm negative polymer functionalized gold nanorods, the chemical images of which can be seen in Fig. 4. Data were obtained in the same manner as described for examples examining nilotinib. The images in Fig. 4 are stacked 2D images, creating a pseudo-3D image that can offer insight into the location and accumulation of particles as a function of depth. No z corrections were made to these data, as no additional information regarding the overall thickness of the cell was obtained.

Cellular incorporation of all particles was confirmed by the co-localization of the gold signal to regions of the cell, as defined by the PC head group. The degree to which uptake occurred was of interest so we could establish the optimal platform for the subsequent nilotinib-functionalized AuNP

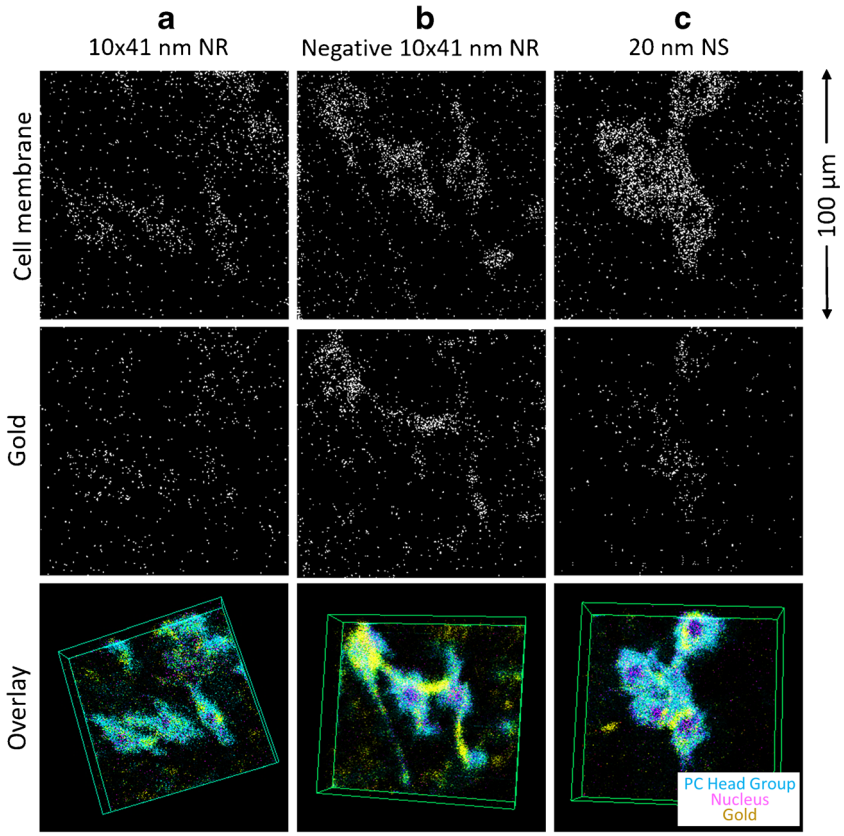

Fig. 4 Positive SIMS chemical images of formalin-fixed RAW 264.7 cells exposed to 10 nm × 41 nm nanorods (*a*), negative 10 nm × 41 nm nanorods (*b*), and 20-nm nanospheres (*c*) overnight. The chemical images showcase the PC head group at *m*/*z* 187.07 and the gold ion at *m*/*z* 196.96. An overlay of these chemical images, with the PC head group in *blue*, the nucleus (*m*/*z* 136.07) in *pink*, and gold in *yellow*, is also shown. The total dose applied for each of these images was 2.8×10^{14} ions per square centimeter. All images are 100 µm × 100 µm

studies. A comparison of gold internalization was performed by our determining the ratio of the ion counts of gold to the counts of the PC head group within the cellular region. A higher ratio indicates increased gold signal.

First, the total ion image was used to determine distinct regions corresponding to a single cell. Only the pixels within this defined area were selected for inspection. Here, the counts within the mass range corresponding to gold (*m*/z 196.96, $\Delta m = 0.025$) were compared with the PC head group ion counts within that region (Table 1). It was found that of the various particles tested, the two nanorods produced the largest gold to PC head group ion count ratio (0.2 ± 0.1 for both 10 nm × 41 nm nanorods and 10 nm × 41 nm negative nanorods). The 20-nm nanospheres were still shown to be internalized at levels above the background, as indicated by ratios in control cells, though the ratios were lower than in the cases involving nanorods.

The chemical images suggest the possibility of aggregation of particles or areas of greater particle accumulation. This aggregation could also serve as an indicator of advantageous uptake, and as such was further explored. Groups of 15 × 15 square pixels were chosen within zones of the cell displaying what appeared to be regions of increased gold uptake (Table 1). Three areas were chosen for each of the nanoparticle studies, and again the ratios between the ion counts of gold and the PC head group ion counts were compared. The negative nanorods showed the highest ratio in the selected pixels (1.2 ± 0.1), demonstrating that these particles are not only taken up more readily but also appear to accumulate or aggregate in larger amounts within a certain cellular regime.

Table 1 Comparison of the ratio of the counts of gold to the counts of the phosphocholine (*PC*) head group in single cell areas to determine which type of nanoparticle exhibits the greatest uptake and 15 × 15 pixels in areas of high "aggregation" of gold signal to determine if increased accumulation was shown from any of the nanoparticle types

	Ratio of Au to PC head group	
	Single cell area	"Aggregated" 15 × 15 pixels within the cell area
10 nm × 41 nm rods	0.2 ± 0.1	0.15 ± 0.03
Negative 10 nm × 41 nm rods	0.2 ± 0.1	1.2 ± 0.1
20-nm spheres	0.09 ± 0.01	0.3 ± 0.1
Control cells	0.03 ± 0.01	NA

NA not available

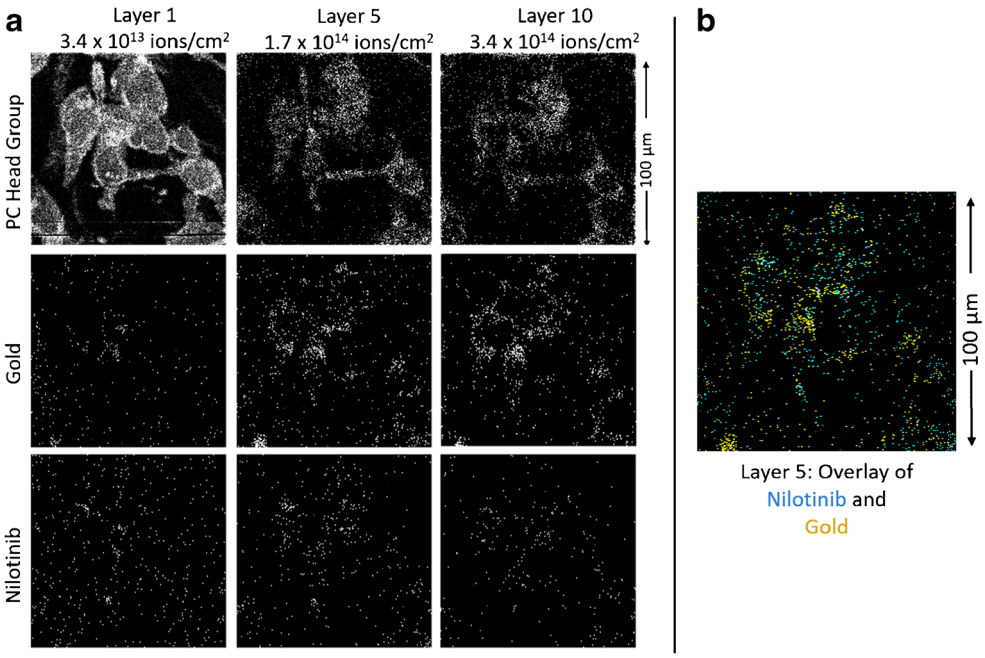

Fig. 5 **a** Positive SIMS chemical images of formalin-fixed RAW 264.7 cells exposed to nilotinib-functionalized gold nanoparticles overnight. The chemical images of the PC head group (*m*/*z* 184.07), gold (*m*/*z* 196.96), and nilotinib (*m*/*z* 530.19) are shown for various depths within the cell. The nilotinib and gold signals are present once the internal regions of the cell have been exposed. These chemical images show the cellular uptake and potential subcellular accumulation of nilotinib-functionalized nanoparticles within these cells. An overlay of nilotinib and gold in layer 5 is shown in **b**. All images are 100 μm × 100 μm

The 20-nm nanospheres were shown to aggregate or accumulate to about the same degree as the 10 nm × 41 nm nanorods.

Nilotinib-functionalized gold nanoparticles

The results of the AuNP uptake experiments prompted the use of 20-nm nanospheres for the platform for nilotinib-functionalized AuNP studies. These nanospheres were chosen over the negative 10 nm × 41 nm nanorods, as the negatively charged functionalization would have proven difficult when nilotinib was being attached.

The nilotinib-functionalized AuNPs were first examined as a dry dropped standard to confirm that both the gold ion and the nilotinib molecular ion could be identified. Once this had been done, RAW 264.7 cells were studied after exposure to these particles. The chemical images can be seen in Fig. 5.

The cellular region is clearly visible, as indicated by the PC head group. The topmost layer of the cells shows small amounts of gold and nilotinib on the surface. This may suggest a slight affinity of the nanoparticle for the exterior regions of the cell. Given the low signal levels, it is also possible that this signal is the result of a partially collapsed cell as a result of formalin fixing.

As portions of the cell are etched away, the interior becomes visible. Here, the gold and the protonated molecular ion of nilotinib are clearly defined and within the confines of the cellular area, meaning that both compounds have been internalized. Although both compounds are co-localized to the cellular region and there are low levels of overlap visually, further analysis was necessary to verify the extent of the co-localization of these compounds. Pixel analysis was done to determine if gold-containing pixels contained nilotinib at higher levels and vice versa, but this was shown not to be the case. Definitive reasons for the lack of correlation between these compounds cannot be stated; however, it is possible that the nilotinib is cleaved from the nanoparticle once it has been internalized or that beam-induced damaged may be causing this lack of co-localization.

The cellular region as a whole was also studied, and it was found that the doped cells contain levels of both gold and nilotinib that are greater than the background signal, as indicated by control cells. Doped cells contain an average of 0.05 ± 0.03 counts of nilotinib per count of PC head group and 0.06 ± 0.03 counts of gold per count of PC head group, whereas control cells contain only background signal of 0.018 ± 0.004 counts of nilotinib per count of PC head group and 0.03 ± 0.01 counts of gold per count of PC head group. This shows that although conclusions regarding the state of the nilotinib-functionalized nanoparticle cannot be drawn, both compounds are internalized within cells and can be measured at levels above the background signal.

Conclusively visualizing both compounds indicates an interaction between the nilotinib and the AuNP carrier that remains at least until the particle is internalized. Although the data do not provide decisive information with respect to the ultimate state of the nilotinib-functionalized nanoparticle, they do illustrate the ability of cluster SIMS to visualize complex pharmaceutical compounds within cells and provide information that may aid in increasing our understanding of the interactions between particles, drugs, and cells.

Conclusions

The ability to use cluster SIMS in the study of the chronic myelogenous leukemia and the Parkinson's drug nilotinib

has been established. This compound can be successfully detected at levels comparable to therapeutic values in single cells. In addition, the data presented here showcase the ability of cluster SIMS to detect various types of AuNPs that could be used for targeted drug therapies. The first example of a cluster SIMS investigation of a model drug-functionalized AuNP has been demonstrated in this study. Unlike with other techniques, both the carrier (AuNP) and the pharmaceutical compound of interest (nilotinib) can be identified intracellularly in one experiment. This ability to successfully determine cellular uptake of both components of functionalized AuNPs paves the way for work investigating the behavior of these components in greater detail. This work serves as a valuable achievement in exploiting the unique properties of cluster SIMS in nanoparticle canvassing and targeted drug therapy applications.

Acknowledgements The generous support and donation of compounds and technical support by Novartis Pharmaceuticals (David Six and Thomas Krucker) is gratefully acknowledged. This project was financially supported by the National Institutes of Health (grant no. 5R01 GM113746-22).

Compliance with ethical standards

Conflict of interest The authors declare that they have no conflict of interest.

References

1. Hann MM, Simpson GL. Intracellular drug concentration and disposition – the missing link? Methods. 2014;68(2):283–5. doi:10.1016/j.ymeth.2014.05.009.
2. Tufts Center for the Study of Drug Development. Outlook 2015. Boston: Tufts Center for the Study of Drug Development; 2015.
3. Morgan P, Van der Graaf PH, Arrowsmith J, Feltner DE, Drummond KS, Wegner CD, et al. Can the flow of medicines be improved? Fundamental pharmacokinetic and pharmacological principles toward improving phase II survival. Drug Discov Today. 2012;17(9-10):419–24. doi:10.1016/j.drudis.2011.12.020.
4. Kim D, Jon S. Gold nanoparticles in image-guided cancer therapy. Inorg Chim Acta. 2012;393:154–64. doi:10.1016/j.ica.2012.07.001.
5. Emerich DF, Thanos CG. Targeted nanoparticle-based drug delivery and diagnosis. J Drug Target. 2007;15(3):163–83. doi:10.1080/10611860701231810.
6. Groneberg DA, Giersig M, Welte T, Pison U. Nanoparticle-based diagnosis and therapy. Curr Drug Targets. 2006;7(6):643–8. doi:10.2174/138945006777435245.
7. Giljohann DA, Seferos DS, Daniel WL, Massich MD, Patel PC, Mirkin CA. Gold nanoparticles for biology and medicine. Angew Chem Int Ed. 2010;49(19):3280–94. doi:10.1002/anie.200904359.
8. Jeong EH, Jung G, Hong CA, Lee H. Gold nanoparticle (AuNP)-based drug delivery and molecular imaging for biomedical applications. Arch Pharm Res. 2014;37(1):53–9. doi:10.1007/s12272-013-0273-5.
9. Wohlfart S, Gelperina S, Kreuter J. Transport of drugs across the blood-brain barrier by nanoparticles. J Control Release. 2012;161(2):264–73. doi:10.1016/j.jconrel.2011.08.017.
10. Male D, Gromnicova R, McQuaid C. Gold nanoparticles for imaging and drug transport to the CNS. Int Rev Neurobiol. 2016;130:155–98. doi:10.1016/bs.irn.2016.05.003.
11. Dasgupta A (2012) In: Dasgupta A (eds) Therapeutic drug monitoring: newer drugs and biomarkers. London: Academic; 2012. p. ix-X
12. Moein MM, El Beqqali A, Abdel-Rehim M. Bioanalytical method development and validation: critical concepts and strategies. J Chromatogr B. 2016. doi:10.1016/j.jchromb.2016.09.028.
13. Passarelli MK, Newman CF, Marshall PS, West A, Gilmore IS, Bunch J, et al. Single-cell analysis: visualizing pharmaceutical and metabolite uptake in cells with label-free 3d mass spectrometry imaging. Anal Chem. 2015;87(13):6696–702. doi:10.1021/acs.analchem.5b00842.
14. Bloom A, Winograd N. Dye-enhanced imaging of mammalian cells with SIMS. Surf Interface Anal. 2014;46:177–80. doi:10.1002/sia.5587.
15. Bloom AN, Tian H, Winograd N. C_{60}-SIMS imaging of nanoparticles within mammalian cells. Biointerphases. 2016;11(2):02A306. doi:10.1116/1.4939463.
16. Haase MF, Grigoriev D, Moehwald H, Tiersch B, Shchukin DG. Nanoparticle modification by weak polyelectrolytes for pH-sensitive pickering emulsions. Langmuir. 2011;27(1):74–82. doi:10.1021/la1027724.
17. Hagenhoff B, Breitenstein D, Tallarek E, Mollers R, Niehuis E, Sperber M, et al. Detection of micro- and nano-particles in animal cells by ToF-SIMS 3D analysis. Surf Interface Anal. 2013;45(1):315–9. doi:10.1002/sia.5141.
18. Tentschert J, Draude F, Jungnickel H, Haase A, Mantion A, Galla S, et al. TOF-SIMS analysis of cell membrane changes in functional impaired human macrophages upon nanosilver treatment. Surf Interface Anal. 2013;45(1):483–5. doi:10.1002/sia.5155.
19. Draude F, Galla S, Pelster A, Tentschert J, Jungnickel H, Haase A, et al. ToF-SIMS and laser-SNMS analysis of macrophages after exposure to silver nanoparticles. Surf Interface Anal. 2013;45(1):286–9. doi:10.1002/sia.4902.
20. Graham DJ, Wilson JT, Lai JJ, Stayton PS, Castner DG. Three-dimensional localization of polymer nanoparticles in cells using ToF-SIMS. Biointerphases. 2016;11(2):02A304. doi:10.1116/1.4934795.
21. Blay JY, von Mehren M. Nilotinib: a novel, selective tyrosine kinase inhibitor. Semin Oncol. 2011;38(2):S3–9. doi:10.1053/j.seminoncol.2011.01.016.
22. Wyse RK, Brundin P, Sherer TB. Nilotinib – differentiating the hope from the hype. J Parkinson Dis. 2016;6(3):519–22. doi:10.3233/Jpd-160904.
23. Pagan F, Hebron M, Valadez EH, Torres-Yaghi Y, Huang X, Mills RR, et al. Nilotinib effects in Parkinson's disease and dementia with Lewy bodies. J Parkinson Dis. 2016;6(3):503–17. doi:10.3233/Jpd-160867.
24. Reinwald M, Schleyer E, Kiewe P, Blau IW, Burmeister T, Pursche S, et al. Efficacy and pharmacologic data of second-generation tyrosine kinase inhibitor nilotinib in BCR-ABL-positive leukemia patients with central nervous system relapse after allogeneic stem cell transplantation. Biomed Res Int. 2014;2014:637059. doi:10.1155/2014/637059.
25. Jesson G, Brisander M, Andersson P, Demirbuker M, Derand H, Lennernas H, et al. Carbon dioxide-mediated generation of hybrid nanoparticles for improved bioavailability of protein kinase inhibitors. Pharm Res. 2014;31(3):694–705. doi:10.1007/s11095-013-1191-4.
26. Cortese B, D'Amone S, Gigli G, Palama IE. Sustained anti-BCR-ABL activity with pH responsive imatinib mesylate loaded PCL nanoparticles in CML cells. Med Chem Commun. 2015;6(1):212–21. doi:10.1039/c4md00348a.
27. Lam ATN, Yoon J, Ganbold EO, Singh DK, Kim D, Cho KH, et al. Adsorption and desorption of tyrosine kinase inhibitor erlotinib on gold nanoparticles. J Colloid Interface Sci. 2014;425:96–101. doi:10.1016/j.jcis.2014.03.032.
28. Labala S, Mandapalli PK, Kurumaddali A, Venuganti VVK. Layer-by-layer polymer coated gold nanoparticles for topical delivery of imatinib mesylate to treat melanoma. Mol Pharm. 2015;12(3):878–88. doi:10.1021/mp5007163.
29. Petrushev B, Boca S, Simon T, Berce C, Frinc I, Dima D, et al. Gold nanoparticles enhance the effect of tyrosine kinase inhibitors in

acute myeloid leukemia therapy. Int J Nanomed. 2016;11:641–60. doi:10.2147/IJN.S94064.
30. Berman ESF, Fortson SL, Checchi KD, Wu L, Felton JS, Wu KJJ, et al. Preparation of single cells for imaging/profiling mass spectrometry. J Am Soc Mass Spectrom. 2008;19(8):1230–6. doi:10.1016/j.jasms.2008.05.006.
31. Rabbani S, Fletcher JS, Lockyer NP, Vickerman JC. Exploring subcellular imaging on the buncher-ToF J105 3D chemical imager. Surf Interface Anal. 2011;43(1-2):380–4. doi:10.1002/sia.3457.
32. Duckett DR, Cameron MD. Metabolism considerations for kinase inhibitors in cancer treatment. Expert Opin Drug Metab Toxicol. 2010;6(10):1175–93. doi:10.1517/17425255.2010.506873.
33. Fletcher JS, Rabbani S, Henderson A, Lockyer NP, Vickerman JC. Three-dimensional mass spectral imaging of HeLa-M cells - sample preparation, data interpretation and visualisation. Rapid Commun Mass Spectrom. 2011;25(7):925–32. doi:10.1002/rcm.4944.
34. Fu D, Zhou J, Zhu WS, Manley PW, Wang YK, Hood T, et al. Imaging the intracellular distribution of tyrosine kinase inhibitors in living cells with quantitative hyperspectral stimulated Raman scattering. Nat Chem. 2014;6(7):615–23. doi:10.1038/Nchem.1961.
35. Robinson MA, Graham DJ, Castner DG. ToF-SIMS depth profiling of cells: z-correction, 3D imaging, and sputter rate of individual NIH/3T3 fibroblasts. Anal Chem. 2012;84(11):4880–5. doi:10.1021/ac300480g.
36. Abumiya M, Takahashi N, Niioka T, Kameoka Y, Fujishima N, Tagawa H, et al. Influence of UGT1A1*6,*27, and*28 Polymorphisms on nilotinib-induced hyperbilirubinemia in Japanese patients with chronic myeloid leukemia. Drug Metab Pharmacokinet. 2014;29(6):449–54. doi:10.2133/dmpk.DMPK-14-RG-031.
37. Faraji AH, Wipf P. Nanoparticles in cellular drug delivery. Bioorg Med Chem. 2009;17(8):2950–62. doi:10.1016/j.bmc.2009.02.043.
38. Kolhar P, Anselmo AC, Gupta V, Pant K, Prabhakarpandian B, Ruoslahti E, et al. Using shape effects to target antibody-coated nanoparticles to lung and brain endothelium. Proc Natl Acad Sci U S A. 2013;110(26):10753–8. doi:10.1073/pnas.1308345110.

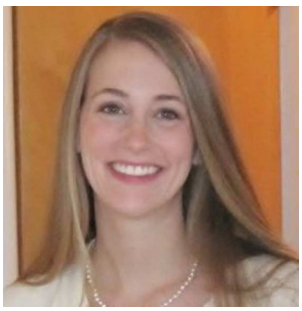

Anna Bloom is a graduate student in the laboratory of Nicholas Winograd at the Pennsylvania State University. Her research has focused on the use of secondary ion mass spectrometry for the imaging of biological systems and the visualization of exogenous compounds within single cells.

Hua Tian is a research associate working in the Winograd group at the Pennsylvania State University. Her work focuses on high-resolution biological imaging using cluster secondary ion mass spectrometry and the development of gas cluster ion beams for the enhancement of ionization and reduction of matrix effects.

Christian Schoen is CEO of Nanopartz Inc., which was founded by him in 2006. The company has become the largest gold nanoparticle supplier to the research industry in the world, selling to more than 2000 customers in more than 30 countries. Its focus is to supply gold and other inorganic nanoparticles to the R & D community while spinning off venture-funded companies that will pursue specific applications in nanotechnology.

Nicholas Winograd is the Evan Pugh University Professor of Chemistry at the Pennsylvania State University. His group focuses on the use of secondary ion mass spectrometry in imaging biomaterials and single cells and studying fundamental aspects of ion/solid interactions and the characterization of solid surfaces.